IEEE Access
Multidisciplinary | Rapid Review | Open Access Journal

Received September 2, 2019, accepted September 9, 2019, date of publication September 17, 2019,
date of current version September 25, 2019.

Digital Object Identifier 10.1109/ACCESS.2019.2940969

Performance Analysis for Cooperative NOMA With Opportunistic Relay Selection

JINJUAN JU[1,2], WEI DUAN[1], QIANG SUN[1], SHANGCE GAO[3], AND GUOAN ZHANG[1]

[1]School of Information Science and Technology, Nantong University, Nantong 226019, China
[2]School of Electronic and Information Engineering, Nantong Vocational University, Nantong 226007, China
[3]Faculty of Engineering, University of Toyama, Toyama 930-8555, Japan

Corresponding author: Guoan Zhang (gzhang@ntu.edu.cn)

This work was supported in part by the National Natural Science Foundation of China under Grant 61971245, Grant 61801249, and Grant 61971467, in part by the Nantong University-Nantong Joint Research Center for Intelligent Information Technology under Grant KFKT2017B01, in part by the Basic Scientific Research of Nantong Science and Technology Project under Grant JCZ18052, and in part by the Natural Science Research Program of Nantong Vocational University under Grant 18ZK01.

ABSTRACT This paper focuses on an effective resource utilization scheme for the cooperative relay selection (RS) system with non-orthogonal multiple access (NOMA). In this work, an opportunistic sub-optimal RS strategy is proposed that considers both of the users; as well as compared with the balanced and random RS schemes. For the proposed effective resource utilization scheme, the relay nodes are selected by incorporating a max-min selection manner to satisfy the quality of service (QoS) of the users; as well as the unselected relays continue receiving the signals transmitted from the base station (BS) for opportunities. In the meanwhile, the selected relay decodes the received superposed signals by employing the successive interference cancellation (SIC), and then reconstructs them into new NOMA signals, which will be forwarded to the users. Moreover, the closed-form expressions in terms of the sum rate (SR) and outage probability of the proposed transmission scheme are derived for independent Rayleigh fading channels. The provided simulation results show that the cooperative NOMA with the proposed effective RS scheme outperforms the existing works, and can also yield a significant performance gain over the orthogonal multiple access (OMA) scheme.

INDEX TERMS Non-orthogonal multiple access (NOMA), cooperative NOMA, relay selection (RS), sum rate (SR), outage probability.

I. INTRODUCTION

Recently, non-orthogonal multiple access (NOMA) has been attracted significant attentions due to its higher spectrum efficiency than the conventional orthogonal multiple access (OMA), which has been recognized as a promising candidate multiple access scheme for future wireless communication networks [1]–[3]. In contrast to the conventional OMA scheme, the key idea of NOMA technique is used to serve multiple users in the same frequency band, but different power levels. To balance user fairness, more power are allocated to the users with poor channel conditions in NOMA scheme, and the system performance is limited by the poor channels [2]. As one of the most effective ways to mitigate the fading effect of the wireless channels in a network, researches in the cooperative transmission receive considerable attentions with the increasing interests in proximity wireless communications.

A few forms of cooperative NOMA schemes have been proposed in the literatures with different issues and channel state information (CSI) assumptions [4]–[11]. In order to improve the spectral efficiency, NOMA with superposition coding is employed in a coordinated system, where the downlink signals from the nearby and cell-edge users are transmitted simultaneously [4], the work shows that the proposed coordinated superposition coding scheme can provide a reasonable transmission rate to a cell-edge user without degrading the rates of the users. By efficiently exploiting prior information transmitted from the users with strong channel conditions, multi-user cooperation is introduced in [5], where the reception reliability for the users with poor connections is also improved. In addition, a cooperative relaying system

The associate editor coordinating the review of this manuscript and approving it for publication was Yulong Zou.

using NOMA is proposed in [6], which not only improves achievable average rate but also reduces the complexity of power allocation. To further reduce the complexity of NOMA system with the coordinated direct and relay transmission, the authors in [7] investigate a novel receiver design by using the inherent property of NOMA that allows one of the receivers to obtain the side information such as undesired data for the interference cancellation, where the performance in terms of the sum-rate (SR) and outage probability are significantly improved. In order to address the ever increasing high capacity demand in wireless heterogeneous networks, a cooperative NOMA technique with successive interference cancellation (SIC) and definition MRC is employed in [8] and [9] to improve the system capacity. Moreover, the works focusing on different channel models, such as Rician fading and Nakagami-*m* fading channels in cooperative NOMA systems, have also been studied in [10] and [11].

To support the requirements of various future Internet of Things scenarios, the works focusing on the combinations of key technologies in 5G, i.e., multiple-input multiple-output [12]–[15], millimetre-wave [16], [17], as well as device-to-device communications [18]–[22] and secure transmissions [23], [24] with NOMA have been widely studied. It is worth noting that, with the expansions of application scenarios and the improvement of system performance, the NOMA networks with multiple relays have been considered. As an effective utilization of resource technique, relay selection (RS) has been considered to reduce the system complexity, as well as remain the full diversity gain for multi-relay networks [25]–[31]. The impact of RS on cooperative NOMA has been studied in [25], where a two-stage RS strategy is proposed, the analytical results demonstrate that the proposed two-stage scheme can achieve not only the optimal diversity gain, but also the minimal outage probability. To meet the different quality of service (QoS) requirements at the users, a new two-stage RS scheme is proposed in [26], where QoS of one user can be strictly satisfied in the first stage, while maximizing the rates of the remained users in the second stage. Unlike the two-stage max-min scheme, in [25], the power allocation coefficients of the users are depended on the relay-destination channels in two-stage decode-and-forward (DF) relaying and they are functions of the source-relay and relay-destination channels in two-stage amplify-and-forward relaying. In [27], the joint user and RS algorithm for cooperative NOMA networks are investigated, where multiple users' messages are transmitted to two destinations by utilizing multiple relays. Considering distributed space-time coding, two-stage dual RS with the fixed power allocation and two-stage dual RS with dynamic power allocation are proposed in [28]. In contrast to the suboptimal user ordering strategy in [25] and [26] that is predefined according to the QoS requirements of the users, the proposed optimal user ordering strategies in [29] are designed adaptively according to the instantaneous CSI. To tackle spectrum efficiency and energy efficiency for randomly deployed users, in [30], the application of simultaneous wireless information and power transfer to NOMA is investigated by using stochastic geometry. The impact of RS on the performance of cooperative NOMA, where relay nodes are capable of working in either full-duplex or half-duplex mode is further investigated [31]. Moreover, to achieve different user fairness levels, an optimal power allocation scheme for sum throughput maximization of NOMA system with α-fairness has been investigated in [32], [33]. To the best of our knowledge, these studies do not pay much attentions to the receptions and information processing of unselected relays during the time slots that selected relays are working, that means, the multiple time slots and relay nodes are not considered with a full utilization.

Based on the above observations, in this paper, a new cooperative transmission NOMA system model with opportunistic suboptimal RS stategy focusing on time-domain is studied. Comparing to the previous half-duplex transmission schemes, the proposed effective transmission scheme is addressed to improve the utilization of resources by forwarding the decoded signals during all the odd time slots. To satisfy the users' different QoS requirements, as well as maximize the sum rate (SR) possibly, the combination of the max-min and proposed opportunistic suboptimal manners is adopted.

The key contributions of this paper are summarized as follows:

- A new multi-relay transmission scheme is investigated in cooperative NOMA system, where the unselected relays are designed to continue receiving the superposed signals transmitted from the BS in the rest time slots, while the selected relay decoding the received superposition signals with SIC and forwarding the reconstructed new NOMA signal. Due to the possibility of improving the performance of the half-duplex DF relaying system, as well as reducing the energy consumption at the transmitters, unlike the conventional schemes, the unselected relay nodes perform signal receptions during all the even time slots for the next opportunities to be selected.
- By comparing RS schemes (max-min RS, opportunistic RS, balanced RS and round robin RS), we characterize the impact of RS strategies on the performance of the proposed cooperative NOMA networks. To achieve the full utilization of time resources, the opportunistic suboptimal RS is adopted after the first max-min RS at the multi-relay layer during the transmission phase. By this way, the users can receive different useful signals form the selected node in each time slot (except the first time slot), which will greatly improve the resource utilization.
- The performance of the proposed scheme in terms of the ergodic SR and outage probability is analysed. Considering independent Rayleigh fading channels, the closed-form expressions of the ergodic SR and outage probability are derived. Simulations support that the derived closed-form expressions of our proposed effective resource utilization scheme outperforms the previous cooperative NOMA and conventional OMA schemes significantly.

The rest of this paper is organized as follows. In Section II, we present the research problem and the improved model. The performance in terms of the ergodic SR, outage probability and some auxiliary indicators are analysed in Section III. Section IV contains the system simulation conditions and results. This paper is concluded in Section V.

II. SYSTEM MODEL AND PROPOSED SCHEME

In this section, we first introduce our proposed system model based on the idea of mobilizing idle time slots and multi-relay resources, and then analyse the feasibility of the effective transmission scheme in the corresponding multi-slot multi-relay scenario. Consider a cooperative multi-relay downlink scenario with one BS, two users, and N relays,[1] where all nodes are operated in a half-duplex DF mode. Each node is equipped with a single antenna. The BS and relays are constrained by the transmitted powers P_t and P_r, respectively. Denote the channels from the BS to relay i and relay i to user j as $h_{SR_i}^{(t_m)}$ and $g_{R_iD_j}^{(t_n)}$ ($i \in \{1, \cdots, N\}$ and $j \in \{1, 2\}$), where t_m and t_n ($1 \leq m < N$ and $n = m + 1$) represent the m-th and n-th time slots. Assume that all channels experience independent and identically Rayleigh fading with variances β_{SR_i} and $\beta_{R_iD_j}$ as their average powers. Moreover, it is also considered that there is no direct link between the BS and users since the users are out of the transmission range of the BS. Furthermore, each relay node is assumed to know the CSI of $h_{SR_i}^{(t_m)}$ and $g_{R_iD_j}^{(t_n)}$ perfectly.

A. PREVIOUS TRANSMISSION SCHEMES

In the previous multi-relay cooperative NOMA transmission networks, each transmission consists of two time slots. During the first time slot, the BS transmits a superposed signal, $S_t = \sum_{j=1}^{2} \sqrt{a_j P_t} s_j$, where s_j is the symbol for the user j, and a_j with $\sum_{j=1}^{2} a_j = 1$ denotes the power allocation coefficient. Similar to the conventional NOMA technology, the power coefficients are related to the qualities of the channels. Without loss of generality, note that $a_1 \geq a_2$, since user 1 is the NOMA-far user whereas user 2 is the near user or the former who has a worse channel condition. The observation at relay i ($1 \leq i \leq N$) is given by

$$y_{R_i}^{(t_1)} = h_{SR_i}^{(t_1)}(\sqrt{a_1 P_t} s_1 + \sqrt{a_2 P_t} s_2) + n_{R_i}^{(t_1)}, \tag{1}$$

where $n_{R_i}^{(t_1)} \sim \mathcal{CN}(0, \sigma_{it_1}^2)$ is the additive white Gaussian noise (AWGN) during the 1-st time slot.

Following NOMA decoding principle, the relays will decode s_1 by treating symbol s_2 as noise, and employing SIC to acquire symbol s_2. In this manner, the received signal-to-interference-plus-noise ratio (SINR) $\gamma_{R_i,s_1}^{(t_1)}$ and signal-to-noise ratio (SNR) $\gamma_{R_i,s_2}^{(t_1)}$ at relay i node are given by

$$\gamma_{R_i,s_1}^{(t_1)} = \frac{\left|h_{SR_i}^{(t_1)}\right|^2 a_1 \rho_i^{(t_1)}}{\left|h_{SR_i}^{(t_1)}\right|^2 a_2 \rho_i^{(t_1)} + 1}, \tag{2}$$

and

$$\gamma_{R_i,s_2}^{(t_1)} = \left|h_{SR_i}^{(t_1)}\right|^2 a_2 \rho_i^{(t_1)}, \tag{3}$$

where $\rho_i^{(t_1)} = \frac{P_t}{\sigma_{ii_1}^2}$ denotes the transmit SNR.

During the second time slot, relay i with the strongest transmission channel coefficient, i.e., an optimal channel group, is selected to decode the signals s_1 and s_2; and then a new superposition coded signal, $S_{R_i} = \sum_{j=1}^{2} \sqrt{b_j P_r} s_j$, is reconstructed and forwarded, where b_j with $\sum_{j=1}^{2} b_j = 1$ denotes the new power allocation coefficient. Similarly, assume that $b_1 \geq b_2$ according to the qualities of the channels.

The criterion for the strongest RS can be written as follows:

$$\max\left\{\min\left\{\left|h_{SR_i}^{(t_1)}\right|^2, \left|g_{R_iD_j}^{(t_2)}\right|^2\right\}, i \in [1, \cdots, N]\right\}, \tag{4}$$

where relay i with the maximum is selected.

The received signal at the user j can be written as

$$y_{D_j}^{(t_2)} = g_{R_iD_j}^{(t_2)}(\sqrt{b_1 P_r} s_1 + \sqrt{b_2 P_r} s_2) + n_{R_iD_j}^{(t_2)}, \tag{5}$$

where $n_{R_iD_j}^{(t_2)}$ is the AWGN at user j during the 2-nd time slot with zero mean and variance $\sigma_{ijt_2}^2$.

To successfully achieve the signal reception and decoding, user 1 will decode the reception with SINR, and user 2 will decode the received message with SNR. Provide that nearby user 2 can decode s_1. Therefore, the corresponding effective SINR and SNR at user j via the selected relay i are given as

$$\gamma_{D_1,s_1}^{(t_2)} = \frac{\left|g_{R_iD_1}^{(t_2)}\right|^2 b_1 \rho_{i1}^{(t_2)}}{\left|g_{R_iD_1}^{(t_2)}\right|^2 b_2 \rho_{i1}^{(t_2)} + 1}, \tag{6}$$

$$\gamma_{D_2,s_1}^{(t_2)} = \frac{\left|g_{R_iD_2}^{(t_2)}\right|^2 b_1 \rho_{i2}^{(t_2)}}{\left|g_{R_iD_2}^{(t_2)}\right|^2 b_2 \rho_{i2}^{(t_2)} + 1}, \tag{7}$$

and

$$\gamma_{D_2,s_2}^{(t_2)} = \left|g_{R_iD_2}^{(t_2)}\right|^2 b_2 \rho_{i2}^{(t_2)}, \tag{8}$$

where $\rho_{ij}^{(t_2)} = \frac{P_r}{\sigma_{ijt_2}^2}$ denotes the transmit SNR in this period.

Considering a multiple time slots N transmission (N is an even number), since that each transmission from the BS to the users via the selected relay involves two time slots, the transmission rate is 0.5. Specifically, on one hand, the unselected relays are idle during the time slot of receiving and decoding performed by the users, and their previous packets play no practical use during the next period; on the other hand, the signal transmitted from the BS is not fully utilized during the whole transmission process, which leads to a certain waste of resources. Clearly, half of the time slots are effectively utilized to transmit signals to the users.

[1] Similar to the research in previous references [25], [26], [28], it is assumed that there is no transmission among relay nodes since that they are out of the service scope with each other. The scenario with interference between relay nodes may set aside for our future work.

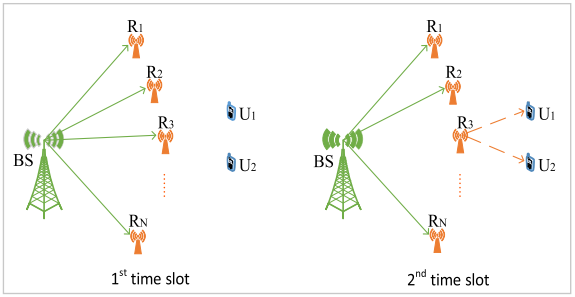

FIGURE 1. The proposed transmission scheme (a).

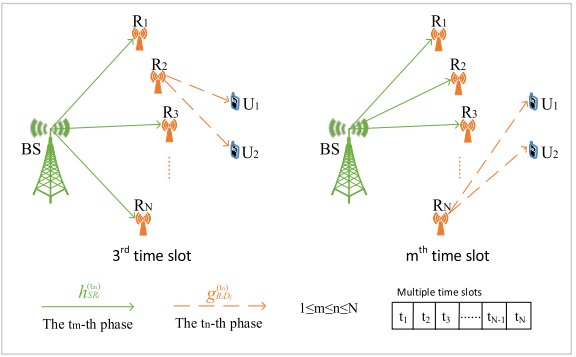

FIGURE 2. The proposed transmission scheme (b).

B. PROPOSED EFFECTIVE TRANSMISSION SCHEME

As a reference to improve resource utilization, the proportion of idle time slots and the use of remained relay nodes are typically considered in the proposed multi-relay cooperative NOMA system. It is necessary to consider a new signal transmission scheme during the rest time slots, especially for the unselected relays. Since it is possible to improve the system performance, as well as reduce the energy consumption at transmitters (the BS and relays), unlike the conventional multi-relay cooperative NOMA networks, a new transmission scheme is proposed in this paper as shown in Figs. 1 and 2.

During the first time slot, similar to the previous scheme, the BS transmits a superposed signal $S_t = \sum_{j=1}^{2} \sqrt{a_j P_t} s_j$ to the relays. The expression for the received signal at each relay is same as Eq. (1).

During the second time slot, assume that relay i (e.g.,3) with the strongest transmission channel coefficients is selected based on criterion (4). As depicted in Fig. 1, the unselected relays continue receiving the signals from the BS, while the selected single relay forwarding the reconstructed SC signals. In this phase, the unselected relays perform signal reception. Denoting $\mathcal{K} = N - 1$, the received signal at the unselected relay k ($k \in \mathcal{K}$), can be expressed as

$$y_{R_k}^{(t_2)} = h_{SR_k}^{(t_2)}(\sqrt{a_1 P_t} s_1 + \sqrt{a_2 P_t} s_2) + n_{R_k}^{(t_2)}, \tag{9}$$

where $n_{R_k}^{(t_2)} \sim \mathcal{CN}(0, \sigma_{kt_2}^2)$ is the AWGN at node k during the second time slot. With (9), the corresponding effective SINR and SNR at relay k for s_1 and s_2 are given by

$$\gamma_{R_k, s_1}^{(t_2)} = \frac{\left|h_{SR_k}^{(t_2)}\right|^2 a_1 \rho_k^{(t_2)}}{\left|h_{SR_k}^{(t_2)}\right|^2 a_2 \rho_k^{(t_2)} + 1}, \tag{10}$$

and

$$\gamma_{R_k, s_2}^{(t_2)} = \left|h_{SR_k}^{(t_2)}\right|^2 a_2 \rho_k^{(t_2)}, \tag{11}$$

where $\rho_k^{(t_2)} = \frac{P_t}{\sigma_{kt_2}^2}$ represents the transmit SNR.

From the view of the signal receptions at the relays and users, the difference between the proposed scheme and previous one begins with time slot 3, some related RS criteria are discussed as follows.

1) OPPORTUNISTIC RS CRITERION

In this phase, an opportunistic suboptimal relay is selected among the unselected relays during the previous time slot according to the evolution of RS criterion, that is

$$\max\left\{\min\left\{\left|h_{SR_k}^{(t_2)}\right|^2, \left|g_{R_k D_j}^{(t_3)}\right|^2\right\}, k \in \mathcal{K}\right\}, \tag{12}$$

where $\mathcal{K} = \{1, \cdots, i-1, i+1, \cdots, N\}$ is represented as $\mathcal{K}$ outage relays except the selected relay i. For users, the expressions of the received signals are similar to the Eq. (5), and the symbol for each user can be decoded.

It is worth pointing out that, the opportunistic RS can be converted into an improved max-min RS, namely, max-max RS, i.e.,

$$\max\left\{\max\left\{\mathcal{F}, \mathcal{G}\right\}\right\}, \tag{13}$$

where $\mathcal{F} = \frac{A+B}{A \cdot B}$ and $\mathcal{G} = \frac{C+D}{C \cdot D}$ are certain expressions referred to the channel qualities based on the definitions in proof. However, Appendix A only describes the procedure of RS for two users. Once relay is selected, the system performance can still be analyzed based on the Eq. (12).

Proof: Please refer to Appendix A.

By using the combination of the max-min and the proposed opportunistic criterions, the opportunities of RS in whole process are more balanced. This manner improves opportunities of the weak relays and reduces heavy burden of a few specific strong relays.

2) BALANCED RS CRITERION

For more reasonable fairness, a balanced selection scheme can be considered according to the statistical method. The balanced factors ϱ_h and ϱ_g are defined as $\frac{|h_k|^2}{E\left[|h_{i'}|^2\right]}$ and $\frac{|g_k|^2}{E\left[|g_{i'}|^2\right]}$, respectively, which will be participated in the implementation of RS. $|h_k|^2/|g_k|^2$ is the channel condition of the current time slot, and $E[|h_{i'}|^2]/E[|g_{i'}|^2]$ denotes the mean channel strength of the previous time slots. Hence, the criterion considering balanced factors, can be written as

$$\max\left\{\min\left\{\varrho_h \left|h_{SR_k}^{(t_2)}\right|^2, \varrho_g \left|g_{R_k D_j}^{(t_3)}\right|^2\right\}, k \in \mathcal{K}\right\}. \tag{14}$$

Predictably, the system performance with the balanced RS criterion is slightly worse than the one with opportunistic RS. The balanced criterion expands the scope of RS for increasing selected opportunities, which reflects a moderate balance between multi-relay nodes; while the opportunistic criterion focuses on the present strong relays for a high system performance.

3) ROUND ROBIN RS CRITERION

From an equal opportunity perspective, a round robin mechanism can be considered. Different from the aforementioned criteria, all relays are selected in turn to transmit received NOMA signals to the users. In this network, the BS firstly sends superposed signal to the relays in time slot 1. And then the selected relay decodes and forwards the new reconstructed NOMA signal. In particular, the relays are selected in turn for working in the following time slots, i.e., 2, 3, $\cdots$, till N. For multi-relay system, the round robin RS criterion works by rotating relay request per period, which can be described as

$$\text{round robin}\left\{\underbrace{R_1, R_2 \cdots R_i \cdots R_N}_{t_1, t_2 \cdots t_i \cdots t_N}\right\}. \tag{15}$$

Obviously, this criterion does not improve the system performance, and is even the worst of the three criteria. However, it can mobilize as many relay nodes as possible for transmission. This phenomenon reflects the fact that effective resource utilization and system performance are mutually restricted and balanced.

As shown in Fig. 2, with criterion (12), the selected relay i' (e.g.,2) continues forwarding the reconstructed signals to the users after decoding the received signal; and, the users employ the technology of SIC to decode the required symbols after receiving; meanwhile, the new unselected relays including previously released DF relay i (e.g.,3) remain receiving signals from the BS. Obviously, the new selected relay i' (e.g.,2) is not the optimum among all relays; however, it can ensure that one more signal reception, i.e., $y_{D_j}^{(t_3)}$, is achieved at user j. The extra reception can be written as

$$y_{D_j}^{(t_3)} = g_{R_k D_j}^{(t_3)}(\sqrt{b_1 P_r} s_1 + \sqrt{b_2 P_r} s_2) + n_{R_k D_j}^{(t_3)}, \tag{16}$$

where $g_{R_k D_j}^{(t_3)}$ denotes the channel gain between the new selected relay k and user j , meanwhile $n_{R_k D_j}^{(t_3)}$ is the AWGN with zero mean and variance $\sigma_{kjt_3}^2$ at user j in time slot 3.

With (16), the corresponding effective SINR and SNR at user j for s_1 and s_2 are given by

$$\gamma_{D_1,s_1}^{(t_3)} = \frac{\left|g_{R_k D_1}^{(t_3)}\right|^2 b_1 \rho_{k1}^{(t_3)}}{\left|g_{R_k D_1}^{(t_3)}\right|^2 b_2 \rho_{k1}^{(t_3)} + 1}, \tag{17}$$

$$\gamma_{D_2,s_1}^{(t_3)} = \frac{\left|g_{R_k D_2}^{(t_3)}\right|^2 b_1 \rho_{k2}^{(t_3)}}{\left|g_{R_k D_2}^{(t_3)}\right|^2 b_2 \rho_{k2}^{(t_3)} + 1}, \tag{18}$$

and

$$\gamma_{D_2,s_2}^{(t_3)} = \left|g_{R_k D_2}^{(t_3)}\right|^2 b_2 \rho_{k2}^{(t_3)}, \tag{19}$$

where $\rho_{kj}^{(t_3)} = \frac{P_r}{\sigma_{kjt_3}^2}$ denotes the transmit SNR in this period.

By this way, it is easy to see that until the last N time slot there are $N/2 - 1$ extra signal receptions at the users during the odd numbers of periods except the first one. Based on the above observations, even that the optimal channels are out of the range due to a half duplex transmission, the opportunistic suboptimal RS will generate an effective utilization of relays to compensate for the loss of system performance. Comparing with the max-min RS scheme where user j receives only one signal for every two time slots, users receive different useful signals in each time slot (after time slot 2), which improves the use of time resources. Hence, for user j, $N-1$ signals are received in summary. In this paper, fixed power allocation is used for each time slot for simplicity. Optimizing the power allocation coefficients can further improve the system performance and reduce energy consumption more reasonably, it is our future works.

Assume that users decode receptions at the end of each time slot by employing SIC. In summary, the transmissions in time slots 1 and 2 of the above schemes follow the same mode throughout the whole process; during the following time slots, from 3 to N, the criteria of RS change, so do the signal receptions of users; hence, the achievable ergodic SR for the proposed scheme, consisting of three parts, can be obtained as (20), where $\mathcal{P}_1$, $\mathcal{P}_2$, and $\mathcal{P}_l$ refer to the received SINR and SNR during time slots 1, 2, and 3 to N, respectively.

$$C_{pro} = \frac{1}{N}\left(\mathcal{P}_1 + \mathcal{P}_2 + \sum_{l=3}^{N} \mathcal{P}_l\right), \tag{20}$$

$\mathcal{P}_1$ is zero since that there is no reception at the users in the first time slot, $\mathcal{P}_2$ is described as (21), as shown at top of the next page and $\mathcal{P}_l$ ($3 \le l \le N$) is similar to $\mathcal{P}_2$ as long as changing the selected relay i into k based on our proposed opportunistic suboptimal RS scheme in any l-th period, $1/N$ means the total transmission periods. For details, C_{pro} is described as Eq. (22), as shown at the top of the next page.

For criteria (14) and (15), the transceiver analyses of the signals are similar to (12), except the weight and the order of selected relays. The performance analysis of system in the next section will be carried out by using criterion (12) for a comparison with the conventional NOMA and the OMA scenarios.

III. PERFORMANCE ANALYSIS

In this section, we will analyze the performance of our proposed effective transmission scheme for independent Rayleigh fading channels in terms of the ergodic SR and the outage probability.

$$\mathcal{P}_2 = \max\left(\log_2\left(1+\min\left\{\gamma_{R_i,s_1}^{(t_1)},\gamma_{D_1,s_1}^{(t_2)},\gamma_{D_2,s_1}^{(t_2)}\right\}\right)+\log_2\left(1+\min\left\{\gamma_{R_i,s_2}^{(t_1)},\gamma_{D_2,s_2}^{(t_2)}\right\}\right)\right) \tag{21}$$

$$\begin{aligned} C_{pro} = \frac{1}{N}\Bigg\{0+\Bigg(\log_2\Bigg(1+\underbrace{\max\left\{\min\left\{\gamma_{R_i,s_1}^{(t_1)},\gamma_{D_1,s_1}^{(t_2)},\gamma_{D_2,s_1}^{(t_2)}\right\}\right\}}_{\mathcal{O}_1}\Bigg)+\log_2\Bigg(1+\underbrace{\max\left\{\min\left\{\gamma_{R_i,s_2}^{(t_1)},\gamma_{D_2,s_2}^{(t_2)}\right\}\right\}}_{\mathcal{O}_2}\Bigg)\Bigg) \\ +\sum_{l=3}^{N}\Bigg(\log_2\Bigg(1+\underbrace{\max\left\{\min\left\{\gamma_{R_k,s_1}^{(t_{l-1})},\gamma_{D_1,s_1}^{(t_l)},\gamma_{D_2,s_1}^{(t_l)}\right\}\right\}}_{\mathcal{Q}_1}\Bigg)+\log_2\Bigg(1+\underbrace{\max\left\{\min\left\{\gamma_{R_k,s_2}^{(t_{l-1})},\gamma_{D_2,s_2}^{(t_l)}\right\}\right\}}_{\mathcal{Q}_2}\Bigg)\Bigg)\Bigg\} \end{aligned} \tag{22}$$

$$\begin{aligned} \mathcal{O}_1 &= \max\left\{\min\left\{\gamma_{R_i,s_1}^{(t_1)},\gamma_{D_1,s_1}^{(t_2)},\gamma_{D_2,s_1}^{(t_2)}\right\}\right\} \\ &= \max\left\{\min\left\{\frac{\beta_{SR_i}^{(t_1)}a_1\rho_i^{(t_1)}}{\beta_{SR_i}^{(t_1)}a_2\rho_i^{(t_1)}+1},\frac{\beta_{R_iD_1}^{(t_2)}b_1\rho_{i1}^{(t_2)}}{\beta_{R_iD_1}^{(t_2)}b_2\rho_{i1}^{(t_2)}+1},\frac{\beta_{R_iD_2}^{(t_2)}b_1\rho_{i2}^{(t_2)}}{\beta_{R_iD_2}^{(t_2)}b_2\rho_{i2}^{(t_2)}+1}\right\}\right\}, \end{aligned} \tag{23}$$

A. ERGODIC SR ANALYSIS

According to shannon's theorem, the achievable rates for signals can always be obtained. With the analysis of the proposed model above, denoting $\left|h_{SR_i}^{(t_1)}\right|^2=\beta_{SR_i}^{(t_1)}$ and $\left|g_{R_iD_j}^{(t_2)}\right|^2=\beta_{R_iD_j}^{(t_2)}$, then we have $\mathcal{O}_1$ and $\mathcal{O}_2$ with the max-min criterion of RS, one of which is on the next page and the other as follows,

$$\begin{aligned} \mathcal{O}_2 &= \max\left\{\min\left\{\gamma_{R_i,s_2}^{(t_1)},\gamma_{D_2,s_2}^{(t_2)}\right\}\right\} \\ &= \max\left\{\min\left\{\beta_{SR_i}^{(t_1)}a_2\rho_i^{(t_1)},\beta_{R_iD_2}^{(t_2)}b_2\rho_{i2}^{(t_2)}\right\}\right\}. \end{aligned} \tag{24}$$

Similarly, we can get $\mathcal{Q}_1$ and $\mathcal{Q}_2$, as shown in Eq. (25), as shown at the top of the next page and Eq. (26).

$$\begin{aligned} \mathcal{Q}_2 &= \max\left\{\min\left\{\gamma_{R_k,s_2}^{(t_{l-1})},\gamma_{D_2,s_2}^{(t_l)}\right\}\right\} \\ &= \max\left\{\min\left\{\beta_{SR_k}^{(t_{l-1})}a_2\rho_k^{(t_{l-1})},\beta_{R_kD_2}^{(t_l)}b_2\rho_{k2}^{(t_l)}\right\}\right\}. \end{aligned} \tag{26}$$

From (23), as shown at the top of this page and (24), the achievable ergodic rates of the signals during time slot 2 can be obtained by the use of complementary cumulative distribution function (CCDF), probability density function (PDF) and complex calculus operations.

Proposition 1: In Appendix B, we derive the closed-form expression of the achievable ergodic rate for s_1 during time slot 2, i.e,

$$C_{(t_2)}^{(s_1)} = -\frac{1}{\ln 2}\cdot\left(e^{\varphi}\cdot\mathrm{Ei}\left(-\varphi\right)-e^{\xi}\cdot\mathrm{Ei}\left(-\xi\right)\right), \tag{27}$$

where $\varphi = \frac{1}{\alpha_{SR_i}^{(t_1)}\rho_i^{(t_1)}}+\frac{1}{\alpha_{R_iD_1}^{(t_2)}\rho_{i1}^{(t_2)}}+\frac{1}{\alpha_{R_iD_2}^{(t_2)}\rho_{i2}^{(t_2)}}$ and $\xi = \frac{1}{a_2\alpha_{SR_i}^{(t_1)}\rho_i^{(t_1)}}+\frac{1}{b_2\alpha_{R_iD_1}^{(t_2)}\rho_{i1}^{(t_2)}}+\frac{1}{b_2\alpha_{R_iD_2}^{(t_2)}\rho_{i2}^{(t_2)}}$.

Proposition 2: In Appendix C, we derive the closed-form expression of the achievable ergodic rate for s_2 during time slot 2 correspondingly, i.e,

$$C_{(t_2)}^{(s_2)} = \frac{1}{\ln 2}\cdot e^{\upsilon}\cdot\left(\mathrm{Ei}\left(-\upsilon\psi-\upsilon\right)-\mathrm{Ei}\left(-\upsilon\right)\right), \tag{28}$$

where $\upsilon = \frac{1}{a_2\alpha_{SR_i}^{(t_1)}\rho_i^{(t_1)}}+\frac{1}{b_2\alpha_{R_iD_2}^{(t_2)}\rho_{i2}^{(t_2)}}$ and $\psi = \min\{\frac{a_1}{a_2},\frac{b_1}{b_2}\}$.

Combing (27) and (28), the closed-form expression of the total achievable rate during time slot 2 can be expressed as

$$\mathcal{P}_2 = C_{(t_2)}^{sum} = C_{(t_2)}^{(s_1)}+C_{(t_2)}^{(s_2)}. \tag{29}$$

By using a similar analysis method, we derive the closed-form expressions of the achievable ergodic rate for s_1 and s_2 during time slot l , as shown in corollary 1 and corollary 2.

Corollary 1: The achievable ergodic rate for s_1 during time slot l is as follows,

$$C_{(t_l)}^{(s_1)} = -\frac{1}{\ln 2}\cdot\left(e^{\varphi'}\cdot\mathrm{Ei}\left(-\varphi'\right)-e^{\xi'}\cdot\mathrm{Ei}\left(-\xi'\right)\right), \tag{30}$$

where $\varphi' = \frac{1}{\alpha_{SR_i}^{(t_{l-1})}\rho_i^{(t_{l-1})}}+\frac{1}{\alpha_{R_iD_1}^{(t_l)}\rho_{i1}^{(t_l)}}+\frac{1}{\alpha_{R_iD_2}^{(t_l)}\rho_{i2}^{(t_l)}}$ and $\xi' = \frac{1}{a_2\alpha_{SR_i}^{(t_{l-1})}\rho_i^{(t_{l-1})}}+\frac{1}{b_2\alpha_{R_iD_1}^{(t_l)}\rho_{i1}^{(t_l)}}+\frac{1}{b_2\alpha_{R_iD_2}^{(t_l)}\rho_{i2}^{(t_l)}}$,

Corollary 2: The achievable ergodic rate for s_2 during time slot l is shown below,

$$C_{(t_l)}^{(s_2)} = \frac{1}{\ln 2}\cdot e^{\upsilon'}\cdot\left(\mathrm{Ei}\left(-\upsilon'\psi-\upsilon'\right)-\mathrm{Ei}\left(-\upsilon'\right)\right), \tag{31}$$

where $\upsilon' = \frac{1}{a_2\alpha_{SR_i}^{(t_{l-1})}\rho_i^{(t_{l-1})}}+\frac{1}{b_2\alpha_{R_iD_2}^{(t_l)}\rho_{i2}^{(t_l)}}$ and $\psi = \min\{\frac{a_1}{a_2},\frac{b_1}{b_2}\}$.

Proof: Please refer to Appendix D.

$$\mathcal{Q}_1 = \max\left\{\min\left\{\gamma_{R_k,s_1}^{(t_{l-1})}, \gamma_{D_1,s_1}^{(t_l)}, \gamma_{D_2,s_1}^{(t_l)}\right\}\right\}$$
$$= \max\left\{\min\left\{\frac{\beta_{SR_k}^{(t_{l-1})} a_1 \rho_k^{(t_{l-1})}}{\beta_{SR_k}^{(t_{l-1})} a_2 \rho_k^{(t_{l-1})} + 1}, \frac{\beta_{R_kD_1}^{(t_l)} b_1 \rho_{k1}^{(t_l)}}{\beta_{R_kD_1}^{(t_l)} b_2 \rho_{k1}^{(t_l)} + 1}, \frac{\beta_{R_kD_2}^{(t_l)} b_1 \rho_{k2}^{(t_l)}}{\beta_{R_kD_2}^{(t_l)} b_2 \rho_{k2}^{(t_l)} + 1}\right\}\right\}, \quad (25)$$

Hence, the closed-form expression of the achievable SR for all l-th ($3 \le l \le N$) periods can be written as (32).

$$\sum_{l=3}^{N} \mathcal{P}_l = \sum_{l=3}^{N} C_{(t_l)}^{sum} = \sum_{l=3}^{N} \left(C_{(t_l)}^{(s_1)} + C_{(t_l)}^{(s_2)}\right). \quad (32)$$

Finally, considering all the periods together, according to (20), combing (29) and (32), the ergodic SR of our proposed system in closed-form can be described as (33).

$$C_{pro} = \frac{1}{N}\left(\mathcal{P}_1 + \mathcal{P}_2 + \sum_{l=3}^{N} \mathcal{P}_l\right)$$
$$= \frac{1}{N}\left(C_{(t_2)}^{(s_1)} + C_{(t_2)}^{(s_2)} + \sum_{l=3}^{N}\left(C_{(t_l)}^{(s_1)} + C_{(t_l)}^{(s_2)}\right)\right)$$
$$= \frac{1}{N}\sum_{n=2}^{N}\left(C_{(t_n)}^{(s_1)} + C_{(t_n)}^{(s_2)}\right). \quad (33)$$

B. OUTAGE PROBABILITY ANALYSIS

According to the QoS rates required by users, each user has a predetermined target data. When the link capacity cannot meet the required user rate, communication interruption will occur. In this section, we will analyze the solutions of the outage probability in our proposed system. Assuming that for s_i the user's target rate is R_{s_i} and the predefined target rate threshold is $R_{\mathcal{T}_{s_i}}$, the outage probability can be described as

$$P_{out} = 1 - \Pr\left\{R_{s_1} > 2^{NR_{\mathcal{T}_{s_1}}} - 1, R_{s_2} > 2^{NR_{\mathcal{T}_{s_2}}} - 1\right\}$$
$$= 1 - \prod_{j=1}^{2} \underbrace{\Pr\left(R_{s_i} > 2^{NR_{\mathcal{T}_{s_i}}} - 1\right)}_{\chi_j}. \quad (34)$$

Further assume that $\omega_i = 2^{NR_{\mathcal{T}_{s_i}}} - 1$ for the sake of simplicity and convenience of analysis, and refer to the above analysis of ergodic SR; therefore, the exact expressions of χ_j can be described as

$$\chi_1 = \Pr\left\{\min\left\{\gamma_{R_k,s_1}^{(t_{l-1})}, \gamma_{D_1,s_1}^{(t_l)}, \gamma_{D_2,s_1}^{(t_l)}\right\} > \omega_1\right\}$$
$$= \Pr\left\{\gamma_{R_k,s_1}^{(t_{l-1})} > \omega_1\right\}\Pr\left\{\gamma_{D_1,s_1}^{(t_l)} > \omega_1\right\}\Pr\left\{\gamma_{D_2,s_1}^{(t_l)} > \omega_1\right\}, \quad (35)$$

i.e.,

and

$$\chi_2 = \Pr\left\{\min\left\{\gamma_{R_k,s_2}^{(t_{l-1})}, \gamma_{D_2,s_2}^{(t_l)}\right\} > \omega_2\right\}$$
$$= \Pr\left\{\gamma_{R_k,s_2}^{(t_{l-1})} > \omega_2\right\}\Pr\left\{\gamma_{D_2,s_2}^{(t_l)} > \omega_2\right\}, \quad (37)$$

i.e.,

$$\chi_2 = \begin{cases} e^{-\frac{\omega_2}{a_2\alpha_{SR_i}^{(t_1)}\rho_i^{(t_1)}} - \frac{\omega_2}{b_2\alpha_{R_iD_2}^{(t_2)}\rho_{i2}^{(t_2)}}}, & \text{for} \quad \omega_2 < \psi, \\ 0, & \text{for} \quad \omega_2 > \psi. \end{cases} \quad (38)$$

By substituting (36), as shown at the bottom of the next page, and (38) back into (34), with the condition $\omega_i < \psi$, the outage probability can be obtained in the closed-form expression as Eq. (39), as shown at the bottom of the next page.

Corollary 3: After some algebraic manipulations, it is easy to see that the diversity order is equal to 1.

Proof: Please refer to Appendix E.

Corollary 4: Since it is significant to discuss the system throughput for delay-limited transmission mode in practical scenarios, similar to [31], it is easy to see that the throughput ceiling is approximately the sum of two targeted date rates, i.e., $\omega_1 + \omega_2$.

Proof: Please refer to Appendix F.

IV. NUMERICAL RESULTS

In this section, we examine the performance of our proposed scheme in terms of the ergodic SR and the outage probability, also compare the performance with previous schemes. For simulation, similar to [34], the following parameters are set: $N = 4$, $\beta_{SR_1} = 8$, $\beta_{SR_2} = 12$, $\beta_{SR_3} = 18$, $\beta_{SR_4} = 10$, and $\beta_{R_1D_1} = \beta_{R_2D_1} = \beta_{R_3D_1} = \beta_{R_4D_1} = 5$, as well as $\beta_{R_1D_2} = \beta_{R_2D_2} = \beta_{R_3D_2} = \beta_{R_4D_2} = 7$. All the numerical results are averaged over 70,000 channel realizations. We study ergodic rates of two signals (s_1 and s_2) and the corresponding SR through a Monte Carlo simulation, then compare obtained analytical results with the simulated ones. The rates of both types match well, as shown in Fig. 3. We investigate ergodic SR performance versus power allocation factors a_i and b_i for our proposed scheme with fixed transmit SNR, as seen in Fig. 4 for two-dimensional and Fig. 5 for three-dimensional. In addition, we investigate the outage performance of our proposed scheme, as demonstrated in Fig. 6, and compare the simulations with the analytical results in three cases. In Fig. 7, we plots the throughput for the proposed RS schemes versus the transmit SNR with different cases involved in Fig. 6. In Figs. 8 and 9, we show the difference of the proposed scheme by employing three criteria, as mentioned in section II. Finally, Fig. 10 illustrates the effective transmission rate versus the transmission time slots, where the comparison is given considering the proposed scheme and conventional schemes.

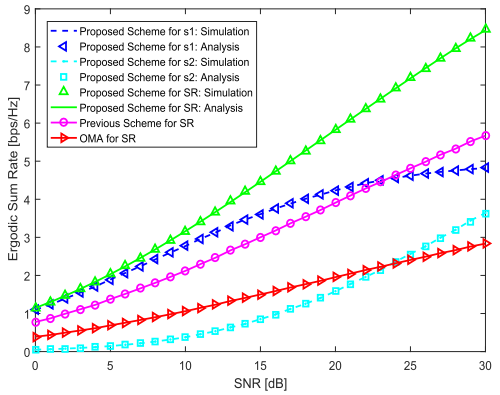

FIGURE 3. The ergodic SRs achieved by three schemes with respect to the transmit SNR.

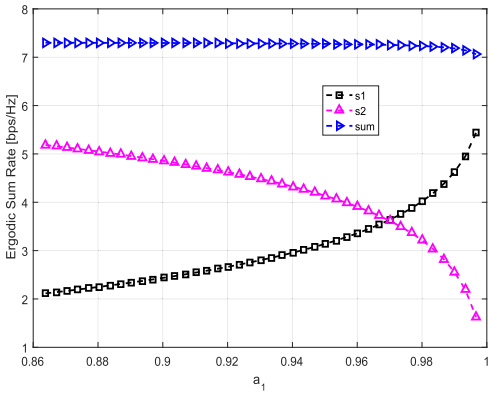

FIGURE 4. The ergodic SRs achieved by our proposed scheme versus different power allocation factor a_1.

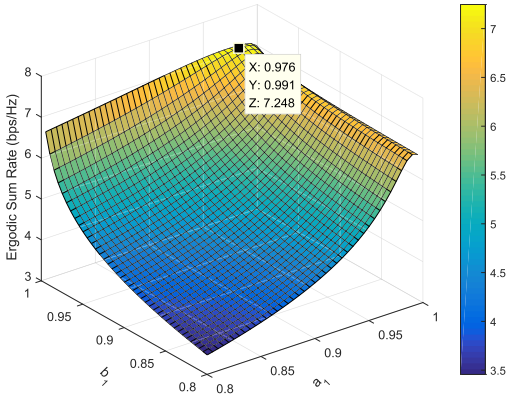

FIGURE 5. The ergodic SRs achieved by our proposed scheme versus different power allocation factors.

A. ERGODIC SR

Fig. 3 depicts the average rates of our proposed effective transmission scheme with fixed $\beta_{SR_i}, \beta_{R_iD_j}$ and corresponding $\alpha_{SR_i}, \alpha_{R_iD_j}$ when $a_1 = 0.99, a_2 = 1 - a_1$, as well as $b_1 = a_1$, $b_2 = a_2$ for simplicity. Clearly, the simulation result either the rate of single signal or the SR of all matches the corresponding analysis result perfectly. Easily, the SR of our proposed scheme has an advantage over the previous and the OMA schemes. Meanwhile, with a increasing SNR, the advantages become more obvious, and the gaps between them at a certain value of SNR become larger. For example, the ergodic SRs are respectively $\{1.066, 2.133, 3.163\}$ bps/Hz where $\rho = 10$ dB and $\{1.954, 3.908, 5.823\}$ bps/Hz where $\rho = 20$ dB. Hence, the gaps are respectively $\{1.030, 1.915\}$ bps/Hz by comparing the proposed scheme with the previous scheme, and $\{2.097, 3.869\}$ bps/Hz by the proposed scheme with the OMA scheme. Predictably, this advantage will become more pronounced with an increasing number of time slots N.

Fig. 4 and Fig. 5 present the ergodic SR performance with respect to power allocation factors a_1 and b_1 for our proposed scheme with fixed transmit SNR as $\rho = 25$ dB. As shown in the figures, optimal values of a_1 and b_1 exist that maximize the ergodic SR. The corresponding a_1 and b_1 for the optimal ergodic SR will be close to 1 as indicated in Fig. 4. Hence, the maximum result of the ergodic SR (7.248 bps/Hz) is obtained with $a_1 = 0.976$ and $b_1 = 0.991$ by using the data cursor in Fig. 5.

B. OUTAGE PROBABILITY

Fig. 6 demonstrates the outage performance of our proposed scheme in terms of the simulation and analytical results with three cases, where the power allocation factors are $a_1 = b_1 = 0.93$, $a_2 = 1 - a_1$, and $b_2 = a_2$. The following system setups are considered similarly as [35]: (1) $\omega_1 = \omega_2 = 0.6$

$$\chi_1 = \begin{cases} e^{-\frac{\omega_1}{\left(a_1\rho_i^{(t_1)} - a_2\rho_i^{(t_1)}\omega_1\right)\alpha_{SR_i}^{(t_1)}} - \frac{\omega_1}{\left(b_1\rho_{i1}^{(t_2)} - b_2\rho_{i1}^{(t_2)}\omega_1\right)\alpha_{R_iD_1}^{(t_2)}} - \frac{\omega_1}{\left(b_1\rho_{i2}^{(t_2)} - b_2\rho_{i2}^{(t_2)}\omega_1\right)\alpha_{R_iD_2}^{(t_2)}}}, & \text{for} \quad \omega_1 < \psi, \\ 0, & \text{for} \quad \omega_1 > \psi; \end{cases} \tag{36}$$

$$\begin{aligned} P_{out} &= 1 - \prod_{j=1}^{2} \underbrace{\Pr\left(R_{s_i} > 2^{NR}\mathcal{T}_{s_i} - 1\right)}_{\chi_j} \\ &= 1 - e^{-\frac{\omega_2}{a_2\alpha_{SR_i}^{(t_1)}\rho_i^{(t_1)}} - \frac{\omega_2}{b_2\alpha_{R_iD_2}^{(t_2)}\rho_{i2}^{(t_2)}}} \\ &\quad e^{-\frac{\omega_1}{\left(a_1\rho_i^{(t_1)} - a_2\rho_i^{(t_1)}\omega_1\right)\alpha_{SR_i}^{(t_1)}} - \frac{\omega_1}{\left(b_1\rho_{i1}^{(t_2)} - b_2\rho_{i1}^{(t_2)}\omega_1\right)\alpha_{R_iD_1}^{(t_2)}} - \frac{\omega_1}{\left(b_1\rho_{i2}^{(t_2)} - b_2\rho_{i2}^{(t_2)}\omega_1\right)\alpha_{R_iD_2}^{(t_2)}}}. \end{aligned} \tag{39}$$

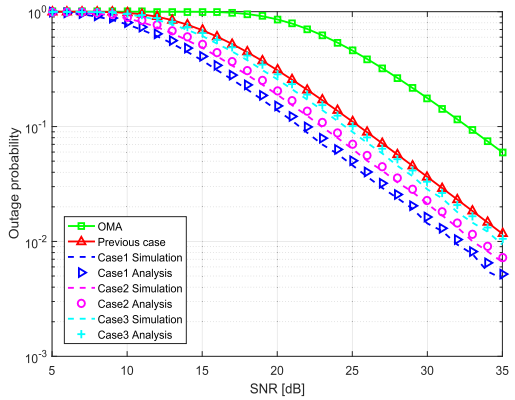

FIGURE 6. The outage probability for three schemes versus the transmit SNR.

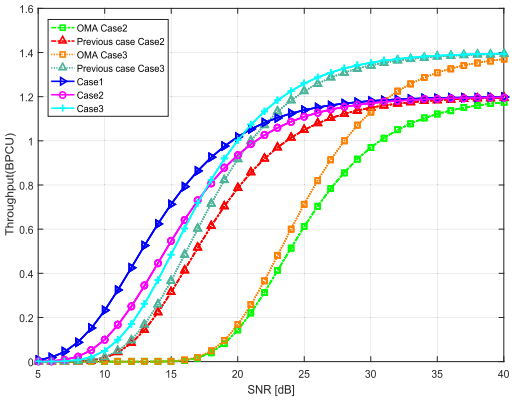

FIGURE 7. The throughput for the proposed RS schemes versus the transmit SNR.

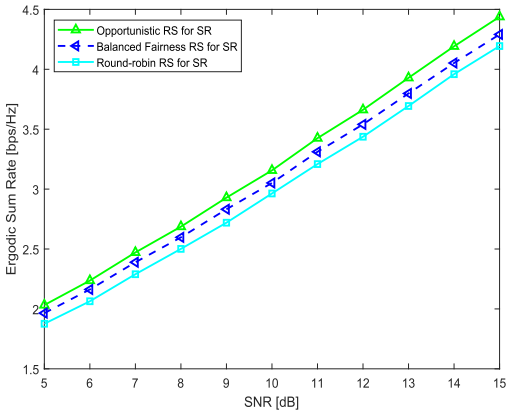

FIGURE 8. The ergodic SRs of our proposed scheme with three RS criteria.

BPCU, $\rho = \{0, 30\}$dB, $\beta_{SR_1} = 8$, $\beta_{SR_2} = 12$, $\beta_{SR_3} = 18$, $\beta_{SR_4} = 10$, and $\beta_{R_1D_1} = \beta_{R_2D_1} = \beta_{R_3D_1} = \beta_{R_4D_1} = 5$, as well as $\beta_{R_1D_2} = \beta_{R_2D_2} = \beta_{R_3D_2} = \beta_{R_4D_2} = 7$ for case 1; (2) $\omega_1 = \omega_2 = 0.6$ BPCU, $\rho = \{0, 30\}$dB, $\beta_{SR_1} = 8$, $\beta_{SR_2} = 12$, $\beta_{SR_3} = 18$, $\beta_{SR_4} = 10$, and $\beta_{R_1D_1} = \beta_{R_2D_1} = \beta_{R_3D_1} = \beta_{R_4D_1} = 3$, as well as $\beta_{R_1D_2} = \beta_{R_2D_2} = \beta_{R_3D_2} = \beta_{R_4D_2} = 4$ for case 2; and (3) $\omega_1 = \omega_2 = 0.7$ BPCU, $\rho = \{0, 30\}$dB, $\beta_{SR_1} = 8$, $\beta_{SR_2} = 12$, $\beta_{SR_3} = 18$, $\beta_{SR_4} = 10$, and $\beta_{R_1D_1} = \beta_{R_2D_1} = \beta_{R_3D_1} = \beta_{R_4D_1} = 3$, as well as $\beta_{R_1D_2} = \beta_{R_2D_2} = \beta_{R_3D_2} = \beta_{R_4D_2} = 4$ for case 3. The results reveal a good match exists between the simulation and analytical results. The outage probabilities of the above three cases change with the transmit SNR. For example, the values are $\{0.1516, 0.2055, 0.2654\}$, where $\rho = 20$ dB, and $\{0.0507, 0.0702, 0.1004\}$ for $\rho = 25$ dB. Clearly, the performance of the outage probability improves as the channel gains increase and the threshold decreases. The former can be observed by comparing case 1 with case 2, while the latter can be shown by comparing case 2 with case 3; hence, case 3 has the worst performance in terms of outage probability.

However, compared with the previous and OMA schemes, all the three cases can efficiently reduce the outage probability. As shown in Fig. 6, the values of case 3 and the above two scenarios are respectively $\{0.2654, 0.3100, 0.8573\}$, where $\rho = 20$ dB and $\{0.1004, 0.1107, 0.4597\}$ where $\rho = 25$ dB. This phenomenon is consistent with our research, hence the proposed effective transmission scheme can offer a significant performance gain over the previous scenarios, especially in terms of the efficiency and reliability.

C. SYSTEM THROUGHPUT

Fig. 7 plots the throughput for the proposed RS schemes versus the transmit SNR with different cases, where the parameters are same to the ones used in Fig. 6. According to Corollary 4 in Section III, it is easy to see that the throughput is subject to the effect of outage probability, and the ceiling is related to the targeted rates. Particularly, with the same sum rate (1.2 BPCU) in both case 1 and 2, a lower outage probability will lead to a higher throughput for the total system. Meanwhile, compared with the previous NOMA and OMA schemes in case 2, the throughput in NOMA-based RS system is significantly improved. It is reasonable, since that due to the fact that the proposed opportunistic RS system can provide more spectrum efficiency than the previous scenarios. Moreover, even the case 3 with the worst outage probability in the three cases leading to a lowest throughput, it will be consistent when the SNR is smaller than 17 dB. However, with a increasing SNR, especially for the high SNR region, the system throughput in case 3 is higher than that of case 2. This is due to the fact that the sum rate has been increased to 1.4 BPCU. To sum up, the proposed scheme overwhelm the other scenarios. Therefore, it is important to select the appropriate transmission rates when designing practical NOMA systems.

D. PERFORMANCE DIFFERENCE

Fig. 8 presents the performance difference in term of SR for our proposed scheme with three RS criteria. Clearly, the opportunistic RS criterion has the best ergodic SR, the round-robin is the worst RS criterion, and the SR of the balanced RS criterion which is between the above two criteria is moderate. Similarly, Fig. 9 shows the distribution of system

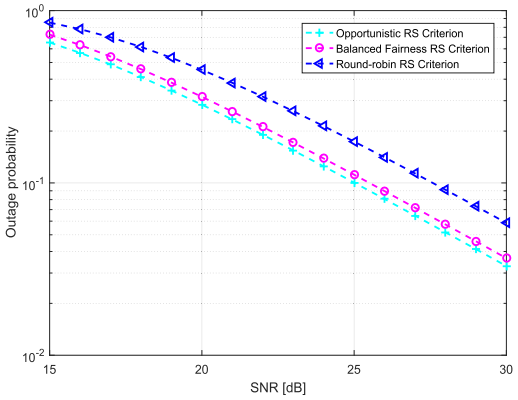

FIGURE 9. The outage probability of our proposed scheme with three RS criteria.

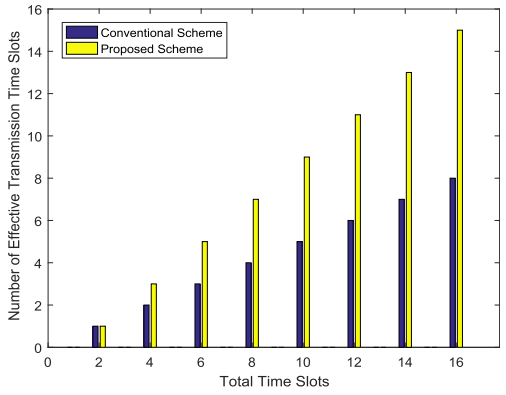

FIGURE 10. Illustration of the rate for our proposed scheme compared with the conventional schemes versus transmission time slots.

outage probability for the criteria. Obviously, the higher the SR of certain scheme is, the lower the corresponding outage probability is. The gaps will be greater with the increasing relay nodes and time slots. Systemic balance is achieved at the expense of performance. We can choose reasonable solution based on system performance requirements in the future.

Fig. 10 illustrates the effective transmission rate versus total time slots by comparing the proposed scheme with conventional one. Considering the utilization of time resources, the proposed scheme is superior to the previous scheme for each number of total time slots, excepted the case for $N = 2$. Since $N - 1$ periods are employed effectively, the transmission rate is $\frac{N-1}{N}$ as discussed in section II. With N increasing, especially, when N goes to infinity, the rate of our proposed scheme will approach to 1; while the value for previous scheme is always 0.5. Hence, the proposed transmission scheme improves the rate of time utilization.

V. CONCLUSION

This paper investigated an effective transmission scheme with RS for the cooperative NOMA. In the scheme, the idea for the receptions at the relay nodes by allowing the unselected relay nodes to continue receiving the superposed signals transmitted from the BS is proposed. In the meanwhile, the new NOMA signals which will be forwarded to the users at the selected relay are reconstructed. The proposed max-min RS is adopted not only to satisfy the different QoS but also to maximize the SR of the two users. Numerical results presented to corroborate the theoretical analyses, and the results shown that the performance in terms of the ergodic SR and outage probability for our proposed scheme gains a significant improvement compared to the conventional NOMA and OMA schemes.

Yet for all that, there are several interesting topics, such as, methods for obtaining CSI, optimal algorithms for power allocation, as well as system security mechanism and attention on different channel models, which remained as our future works.

A. PROOF OF MAX-MAX RS

For simplicity, we define some parameters as follows,

$$\begin{cases} A \triangleq \dfrac{\left|h_{SR}^{(t_\tau)}\right|^2 a_1 \rho^{(t_\tau)}}{\left|h_{SR}^{(t_\tau)}\right|^2 a_2 \rho^{(t_\tau)} + 1}, \\ B \triangleq \left|h_{SR}^{(t_\tau)}\right|^2 a_2 \rho^{(t_\tau)}, \\ C \triangleq \dfrac{\left|g_{RD_1}^{(t_{\tau+1})}\right|^2 b_1 \rho_1^{(t_{\tau+1})}}{\left|g_{RD_1}^{(t_{\tau+1})}\right|^2 b_2 \rho_1^{(t_{\tau+1})} + 1}, \\ D \triangleq \left|g_{RD_2}^{(t_{\tau+1})}\right|^2 b_2 \rho_2^{(t_{\tau+1})}. \end{cases} \tag{A.1}$$

According to Shannon's theorem, the ergodic SRs for users 1 and 2 can be expressed as

$$\begin{cases} F' = \dfrac{1}{2} \cdot \log_2(1 + A) + \dfrac{1}{2} \cdot \log_2(1 + B), \\ G' = \dfrac{1}{2} \cdot \log_2(1 + C) + \dfrac{1}{2} \cdot \log_2(1 + D), \end{cases} \tag{A.2}$$

where F' denotes the SR at relay node, while G' represents the SR at users. Since that the SRs are expected as large as possible, and then the channel for each node is determined by the minimum of the expected maximum of F' and G'. Moreover, relay is selected by searching for the maximum among unselected relay nodes. In summary, since the *max min* $\{SR\}$ aims to obtain the maximum SRs, this problem can be seen as *max min max*, i.e.,

$$\max \left\{ \min \left\{ \max \underbrace{(R\ SR_1)}_{F'}, \ \max \underbrace{(D\ SR_2)}_{G'} \right\} \right\}. \tag{A.3}$$

It is easy to see that $max\{min\{max\{F'\},\ max\{G'\}\}\}$ can be equivalent to $max\{min\{max(1 + A)(1 + B),\ max(1 + C)(1 + D)\}\}$. From that of the rules for optimization, $max(1 + A)(1 + B)$ can be equivalent to $min(\frac{1}{A} + \frac{1}{B})$, therefore the problem can be converted into the one

as follows,

$$\max\left\{\min\left\{\max(1+A)(1+B),\ \max(1+C)(1+D)\right\}\right\}$$
$$\Rightarrow \max\left\{\max\left\{\min(\frac{1}{A}+\frac{1}{B}),\ \min(\frac{1}{C}+\frac{1}{D})\right\}\right\}$$
$$\Rightarrow \max\left\{\max\left\{\mathcal{F},\ \mathcal{G}\right\}\right\}, \tag{A.4}$$

where $\mathcal{F}=\frac{A+B}{A\cdot B}$ and $\mathcal{G}=\frac{C+D}{C\cdot D}$ are the minimums respectively, reflecting the influence of channel qualities, power allocation coefficients and transmit powers.

B. PROOF OF PROPOSITION 1

From (23), the complementary cumulative distribution function (CCDF) of $\mathcal{O}_1$ can be formulated as (B.1).

$$\overline{F}_{\mathcal{O}_1}(o_1)=\Pr\left\{\frac{\beta_{SR_i}^{(t_1)}a_1\rho_i^{(t_1)}}{\beta_{SR_i}^{(t_1)}a_2\rho_i^{(t_1)}+1}>o_1,\ \frac{\beta_{R_iD_1}^{(t_2)}b_1\rho_{i1}^{(t_2)}}{\beta_{R_iD_1}^{(t_2)}b_2\rho_{i1}^{(t_2)}+1}>o_1,\ \frac{\beta_{R_iD_2}^{(t_2)}b_1\rho_{i2}^{(t_2)}}{\beta_{R_iD_2}^{(t_2)}b_2\rho_{i2}^{(t_2)}+1}>o_1\right\}. \tag{B.1}$$

Noting that the CCDF of $\overline{F}_{\beta_\delta}(x)=e^{-\frac{x}{\alpha_\delta}}$, for $\delta\in\{SR_i,R_iD_j\}$, equation (B.1) is equivalent to (B.2) as shown below, when $o_1<\frac{a_1}{a_2}$ and $o_1<\frac{b_1}{b_2}$.

$$\begin{aligned}\overline{F}_{\mathcal{O}_1}(o_1)&=\overline{F}_{SR_i^{(t_1)}}(\frac{o_1}{a_1\rho_i^{(t_1)}-a_2\rho_i^{(t_1)}o_1})\overline{F}_{R_iD_1^{(t_2)}}(\frac{o_1}{b_1\rho_{i1}^{(t_2)}-b_2\rho_{i1}^{(t_2)}o_1})\\&\quad\times\overline{F}_{R_iD_2^{(t_2)}}(\frac{o_1}{b_1\rho_{i2}^{(t_2)}-b_2\rho_{i2}^{(t_2)}o_1})\\&=e^{-\frac{o_1}{\left(b_1\rho_{i1}^{(t_2)}-b_2\rho_{i1}^{(t_2)}o_1\right)\alpha_{R_iD_1}^{(t_2)}}-\frac{o_1}{\left(b_1\rho_{i2}^{(t_2)}-b_2\rho_{i2}^{(t_2)}o_1\right)\alpha_{R_iD_2}^{(t_2)}}}\\&\quad\times e^{-\frac{o_1}{\left(a_1\rho_i^{(t_1)}-a_2\rho_i^{(t_1)}o_1\right)\alpha_{SR_i}^{(t_1)}}},\end{aligned} \tag{B.2}$$

For the case $o_1>\frac{a_1}{a_2}$ and $o_1>\frac{b_1}{b_2}$, $\overline{F}_{\mathcal{O}_1}(o_1)=0$ always holds, since

$$\frac{a_1\beta_{SR_i}^{(t_1)}\rho_i^{(t_1)}}{a_2\beta_{SR_i}^{(t_1)}\rho_i^{(t_1)}+1}<\frac{a_1}{a_2}, \tag{B.3}$$

$$\frac{b_1\beta_{R_iD_1}^{(t_2)}\rho_{i1}^{(t_2)}}{b_2\beta_{R_iD_1}^{(t_2)}\rho_{i1}^{(t_2)}+1}<\frac{b_1}{b_2}, \tag{B.4}$$

and

$$\frac{b_1\beta_{R_iD_2}^{(t_2)}\rho_{i2}^{(t_2)}}{b_2\beta_{R_iD_2}^{(t_2)}\rho_{i2}^{(t_2)}+1}<\frac{b_1}{b_2}. \tag{B.5}$$

With (B.2), by using the equality

$$\int_0^\infty\log_2(1+x)f_X(x)dx=\frac{1}{\ln 2}\int_0^\infty\frac{1-F(x)}{1+x}dx, \tag{B.6}$$

and $F_X(x)=1-\overline{F}_X(x)$, the achievable ergodic rate for s_1 during the second time slot transmission can be calculated as shown in equation (B.7), where denoting $\phi=\frac{1}{\mathcal{A}\alpha_{SR_i}^{(t_1)}}+\frac{1}{\mathcal{B}\alpha_{R_iD_1}^{(t_2)}}+\frac{1}{\mathcal{C}\alpha_{R_iD_2}^{(t_2)}}=\frac{1}{\left(a_1\rho_i^{(t_1)}-a_2\rho_i^{(t_1)}o_1\right)\alpha_{SR_i}^{(t_1)}}+\frac{1}{\left(b_1\rho_{i1}^{(t_2)}-b_2\rho_{i1}^{(t_2)}o_1\right)\alpha_{R_iD_1}^{(t_2)}}+\frac{1}{\left(b_1\rho_{i2}^{(t_2)}-b_2\rho_{i2}^{(t_2)}o_1\right)\alpha_{R_iD_2}^{(t_2)}}$ and $\psi=\min\{\frac{a_1}{a_2},\frac{b_1}{b_2}\}$ for simplification.

$$\begin{aligned}C_{(t_2)}^{(s_1)}&=\int_0^\psi\log_2(1+o_1)dF_{\mathcal{O}_1}(o_1)+\log_2(1+\psi)(1-F_{\mathcal{O}_1}(\psi))\\&=\log_2(1+\psi)-\frac{1}{\ln 2}\int_0^\psi\frac{1}{1+o_1}\left(1-\overline{F}_{\mathcal{O}_1}(o_1)\right)do_1\\&=\int_0^\psi\frac{1}{\ln 2(1+o_1)}e^{-\frac{o_1}{\left(a_1\rho_i^{(t_1)}-a_2\rho_i^{(t_1)}o_1\right)\alpha_{SR_i}^{(t_1)}}}\\&\quad\times e^{-\frac{o_1}{\left(b_1\rho_{i1}^{(t_2)}-b_2\rho_{i1}^{(t_2)}o_1\right)\alpha_{R_iD_1}^{(t_2)}}-\frac{o_1}{\left(b_1\rho_{i2}^{(t_2)}-b_2\rho_{i2}^{(t_2)}o_1\right)\alpha_{R_iD_2}^{(t_2)}}}do_1\\&=\int_0^\psi\frac{1}{\ln 2(1+o_1)}e^{-\frac{o_1}{\mathcal{A}\alpha_{SR_i}^{(t_1)}}-\frac{o_1}{\mathcal{B}\alpha_{R_iD_1}^{(t_2)}}-\frac{o_1}{\mathcal{C}\alpha_{R_iD_2}^{(t_2)}}}do_1\\&=\frac{1}{\ln 2}\int_0^\psi\frac{1}{(1+o_1)}e^{-o_1\phi}do_1,\end{aligned} \tag{B.7}$$

According to $x=\frac{o_1}{\mathcal{A}}=\frac{o_1}{a_1\rho_i^{(t_1)}-a_2\rho_i^{(t_1)}o_1}$, $y=\frac{o_1}{\mathcal{B}}=\frac{o_1}{b_1\rho_{i1}^{(t_2)}-b_2\rho_{i1}^{(t_2)}o_1}$, and $z=\frac{o_1}{\mathcal{C}}=\frac{o_1}{b_1\rho_{i2}^{(t_2)}-b_2\rho_{i2}^{(t_2)}o_1}$ for substitution of variable o_1, then we have

$$\begin{aligned}\mathcal{A}'&=\int_0^\psi\frac{e^{-\frac{o_1}{\mathcal{A}\alpha_{SR_i}^{(t_1)}}}}{o_1+1}do_1\\&=\int_0^\infty e^{\frac{-x}{\alpha_{SR_i}^{(t_1)}}}\left(\frac{1}{x+\frac{1}{\rho_i^{(t_1)}}}+\frac{-1}{x+\frac{1}{a_2\rho_i^{(t_1)}}}\right)dx,\end{aligned} \tag{B.8}$$

$$\begin{aligned}\mathcal{B}'&=\int_0^\psi\frac{e^{-\frac{o_1}{\mathcal{B}\alpha_{R_iD_1}^{(t_2)}}}}{o_1+1}do_1\\&=\int_0^\infty e^{\frac{-y}{\alpha_{R_iD_1}^{(t_2)}}}\left(\frac{1}{y+\frac{1}{\rho_{i1}^{(t_2)}}}+\frac{-1}{y+\frac{1}{b_2\rho_{i1}^{(t_2)}}}\right)dy,\end{aligned} \tag{B.9}$$

and

$$\begin{aligned}\mathcal{C}'&=\int_0^\psi\frac{e^{-\frac{o_1}{\mathcal{C}\alpha_{R_iD_2}^{(t_2)}}}}{o_1+1}do_1\\&=\int_0^\infty e^{\frac{-z}{\alpha_{R_iD_2}^{(t_2)}}}\left(\frac{1}{z+\frac{1}{\rho_{i2}^{(t_2)}}}+\frac{-1}{z+\frac{1}{b_2\rho_{i2}^{(t_2)}}}\right)dz.\end{aligned} \tag{B.10}$$

Using the integral result of exponential functions

$$\int_0^\infty\frac{e^{-\mu x}dx}{x+\beta}=e^{\mu\beta}\mathrm{Ei}(-\mu\beta) \tag{B.11}$$

[36, Eq. (3.352.4)], formula (B.7) can be equivalently written as (B.12), where $\mathrm{Ei}(\cdot)$ denotes the exponential

integral function.

$$
\begin{aligned}
C_{(t_2)}^{(s_1)} &= \frac{1}{\ln 2}\int_0^{\psi}\frac{1}{(1+o_1)}e^{-\frac{o_1}{\mathcal{A}\alpha_{SR_i}^{(t_1)}}-\frac{o_1}{\mathcal{B}\alpha_{R_iD_1}^{(t_2)}}-\frac{o_1}{\mathcal{C}\alpha_{R_iD_2}^{(t_2)}}}do_1\\
&= \frac{1}{\ln 2}\left(\mathcal{A}'+\mathcal{B}'+\mathcal{C}'\right)\\
&= -\frac{1}{\ln 2}\cdot\Bigg(e^{\left(\frac{1}{\rho_i^{(t_1)}\alpha_{SR_i}^{(t_1)}}+\frac{1}{\rho_{i1}^{(t_2)}\alpha_{R_iD_1}^{(t_2)}}+\frac{1}{\rho_{i2}^{(t_2)}\alpha_{R_iD_2}^{(t_2)}}\right)}\\
&\quad\cdot\Big(\mathrm{Ei}\big(-\big(\frac{1}{\rho_i^{(t_1)}\alpha_{SR_i}^{(t_1)}}+\frac{1}{\rho_{i1}^{(t_2)}\alpha_{R_iD_1}^{(t_2)}}+\frac{1}{\rho_{i2}^{(t_2)}\alpha_{R_iD_2}^{(t_2)}}\big)\big)\Big)\\
&\quad-e^{\left(\frac{1}{a_2\rho_i^{(t_1)}\alpha_{SR_i}^{(t_1)}}+\frac{1}{b_2\rho_{i1}^{(t_2)}\alpha_{R_iD_1}^{(t_2)}}+\frac{1}{b_2\rho_{i2}^{(t_2)}\alpha_{R_iD_2}^{(t_2)}}\right)}\\
&\quad\cdot\Big(\mathrm{Ei}\big(-\big(\frac{1}{a_2\rho_i^{(t_1)}\alpha_{SR_i}^{(t_1)}}+\frac{1}{b_2\rho_{i1}^{(t_2)}\alpha_{R_iD_1}^{(t_2)}}+\frac{1}{b_2\rho_{i2}^{(t_2)}\alpha_{R_iD_2}^{(t_2)}}\big)\big)\Big)\Bigg)
\end{aligned}
\tag{B.12}
$$

C. PROOF OF PROPOSITION 2

For $\mathcal{O}_2$ described in (24), we have

$$
\begin{aligned}
\overline{F}_{\mathcal{O}_2}(o_2) &= \Pr\left\{\beta_{SR_i}^{(t_1)}a_2\rho_i^{(t_1)} > o_2, \beta_{R_iD_2}^{(t_2)}b_2\rho_{i2}^{(t_2)} > o_2\right\}\\
&= \overline{F}_{SR_i^{(t_1)}}\left(\frac{o_2}{a_2\rho_i^{(t_1)}}\right)\times\overline{F}_{R_iD_2^{(t_2)}}\left(\frac{o_2}{b_2\rho_{i2}^{(t_2)}}\right)\\
&= e^{-o_2\left(\frac{1}{a_2\alpha_{SR_i}^{(t_1)}\rho_i^{(t_1)}}+\frac{1}{b_2\alpha_{R_iD_2}^{(t_2)}\rho_{i2}^{(t_2)}}\right)}
\end{aligned}
\tag{C.1}
$$

By taking derivative of (C.1), the probability density function of $\mathcal{O}_2$ can be obtained as

$$
f_{\mathcal{O}_2}(o_2) = -\xi' e^{-o_2\xi'}, \tag{C.2}
$$

where $\xi' = \frac{1}{a_2\alpha_{SR_i}^{(t_1)}\rho_i^{(t_1)}}+\frac{1}{b_2\alpha_{R_iD_2}^{(t_2)}\rho_{i2}^{(t_2)}}$. From (C.1) and (C.2), the achievable ergodic rate for s_2 during time slot 2 can be calculated as

$$
\begin{aligned}
C_{(t_2)}^{(s_2)} &= \frac{1}{\ln 2}\int_0^{\psi}\frac{e^{-o_2\left(\frac{1}{a_2\alpha_{SR_i}^{(t_1)}\rho_i^{(t_1)}}+\frac{1}{b_2\alpha_{R_iD_2}^{(t_2)}\rho_{i2}^{(t_2)}}\right)}}{1+o_2}do_2\\
&= \frac{1}{\ln 2}\int_0^{\psi}\frac{1}{1+o_2}e^{-o_2\xi'}do_2\\
&= \frac{1}{\ln 2}\cdot e^{\xi'}\cdot\Big(\mathrm{Ei}\left(-\xi'\psi-\xi'\right)-\mathrm{Ei}\left(-\xi'\right)\Big),
\end{aligned}
\tag{C.3}
$$

where the integral result

$$
\int_0^u\frac{e^{-\mu x}}{x+\beta}dx = e^{\mu\beta}\left[\mathrm{Ei}(-\mu u-\mu\beta)-\mathrm{Ei}(-\mu\beta)\right] \tag{C.4}
$$

[36, Eq. (3.352.1)] is used, and $\mathrm{Ei}(\cdot)$ denotes the exponential integral function.

D. PROOF OF COROLLARIES 1 AND 2

From (25) and (26), relay i has been changed into relay k during periods $t_{(l-1)}$ and t_l, the achievable rate for s_1 can be formulated as (D.1); while for s_2 can be obtained as (D.2),

$$
\begin{aligned}
&C_{(t_l)}^{(s_1)}\\
&= \frac{1}{\ln 2}\int_0^{\psi}\frac{1}{1+o_1}e^{-\frac{o_1}{\mathcal{A}\alpha_{SR_i}^{(t_{l-1})}}-\frac{o_1}{\mathcal{B}\alpha_{R_iD_1}^{(t_l)}}-\frac{o_1}{\mathcal{C}\alpha_{R_iD_2}^{(t_l)}}}do_1\\
&= -\frac{1}{\ln 2}\cdot\Bigg(e^{\left(\frac{1}{\rho_i^{(t_{l-1})}\alpha_{SR_i}^{(t_{l-1})}}+\frac{1}{\rho_{i1}^{(t_l)}\alpha_{R_iD_1}^{(t_l)}}+\frac{1}{\rho_{i2}^{(t_l)}\alpha_{R_iD_2}^{(t_l)}}\right)}\\
&\quad\cdot\Big(\mathrm{Ei}\big(-\big(\frac{1}{\rho_i^{(t_{l-1})}\alpha_{SR_i}^{(t_{l-1})}}+\frac{1}{\rho_{i1}^{(t_l)}\alpha_{R_iD_1}^{(t_l)}}+\frac{1}{\rho_{i2}^{(t_l)}\alpha_{R_iD_2}^{(t_l)}}\big)\big)\Big)\\
&\quad-e^{\left(\frac{1}{a_2\rho_i^{(t_{l-1})}\alpha_{SR_i}^{(t_{l-1})}}+\frac{1}{b_2\rho_{i1}^{(t_l)}\alpha_{R_iD_1}^{(t_l)}}+\frac{1}{b_2\rho_{i2}^{(t_l)}\alpha_{R_iD_2}^{(t_l)}}\right)}\\
&\quad\cdot\Big(\mathrm{Ei}\big(-\big(\frac{1}{a_2\rho_i^{(t_{l-1})}\alpha_{SR_i}^{(t_{l-1})}}+\frac{1}{b_2\rho_{i1}^{(t_l)}\alpha_{R_iD_1}^{(t_l)}}+\frac{1}{b_2\rho_{i2}^{(t_l)}\alpha_{R_iD_2}^{(t_l)}}\big)\big)\Big)\Bigg)
\end{aligned}
\tag{D.1}
$$

$$
\begin{aligned}
&C_{(t_l)}^{(s_2)}\\
&= \frac{1}{\ln 2}\int_0^{\psi}\frac{e^{-o_2\left(\frac{1}{a_2\alpha_{SR_k}^{(t_{l-1})}\rho_k^{(t_{l-1})}}+\frac{1}{b_2\alpha_{R_kD_2}^{(t_l)}\rho_{k2}^{(t_l)}}\right)}}{1+o_2}do_2\\
&= \frac{1}{\ln 2}\int_0^{\psi}\frac{1}{1+o_2}e^{-o_2\upsilon'}do_2\\
&= \frac{1}{\ln 2}\cdot e^{\upsilon'}\cdot\Big(\mathrm{Ei}\left(-\upsilon'\psi-\upsilon'\right)-\mathrm{Ei}\left(-\upsilon'\right)\Big)
\end{aligned}
\tag{D.2}
$$

where $\upsilon' = \frac{1}{a_2\alpha_{SR_k}^{(t_{l-1})}\rho_k^{(t_{l-1})}}+\frac{1}{b_2\alpha_{R_kD_2}^{(t_l)}\rho_{k2}^{(t_l)}}$ and $\psi = \min\{\frac{a_1}{a_2}, \frac{b_1}{b_2}\}$.

E. PROOF OF COROLLARY 3

The diversity order can be expressed as

$$
\begin{aligned}
d &= -\lim_{\rho\to\infty}\frac{\log(P_{out}(\rho))}{\log\rho}\\
&= -\lim_{\rho\to\infty}\frac{\log(1-e^{-\frac{\mathcal{H}}{\rho}})}{\log\rho},
\end{aligned}
\tag{E.1}
$$

where $P_{out}(\rho)$ is the asymptotic outage probability when $\rho\to\infty$ and $\mathcal{H}$ is the parameter extracted from the exponential function of the outage probability in Eq. (39). From $\lim_{x\to 0}e^{-x}\sim 1-x$, the diversity order can be approximated in the high SNR region as

$$
d \sim -\lim_{\rho\to\infty}\frac{\log(\frac{\mathcal{H}}{\rho})}{\log\rho}. \tag{E.2}
$$

For infinite ρ, $\mathcal{H}$ is negligible, hence, the diversity order in this work is 1.

F. PROOF OF COROLLARY 4

To gain more insights for proposed RS schemes, the throughput analysis can be provided in the high SNR region. According to the derived outage probability of Eq. (39),

the throughput of the proposed schemes can be expressed as [31],

$$\begin{aligned} T &= \left(1 - P_{out}(\rho)\right) \omega_1 + \left(1 - P_{out}(\rho)\right) \omega_2 \\ &= \left(1 - (1 - e^{-\frac{\mathcal{H}}{\rho}})\right) (\omega_1 + \omega_2) \\ &= e^{-\frac{\mathcal{H}}{\rho}} (\omega_1 + \omega_2), \end{aligned} \tag{F.1}$$

where $P_{out}(\rho)$, $\mathcal{H}$ and $\lim_{x \to 0} e^{-x} \sim 1 - x$ are similar to the above proof, considering the high transmit SNR, the throughput can be approximately converted into the following form as

$$T \sim \lim_{\rho \to \infty} \left(1 - \frac{\mathcal{H}}{\rho}\right) (\omega_1 + \omega_2). \tag{F.2}$$

For a large ρ, the term $\mathcal{H}/\rho$ is negligible, which approximately results in the sum of two targeted date rates for the objective throughput T, i.e., $\omega_1 + \omega_2$.

REFERENCES

[1] Y. Saito, Y. Kishiyama, A. Benjebbour, T. Nakamura, A. Li, and K. Higuchi, "Non-orthogonal multiple access (NOMA) for cellular future radio access," in *Proc. IEEE Veh. Technol. Conf.*, Dresden, Germany, Jun. 2013, pp. 1–5.

[2] Z. Ding, Z. Yang, P. Fan, and H. V. Poor, "On the performance of non-orthogonal multiple access in 5G systems with randomly deployed users," *IEEE Signal Process. Lett.*, vol. 21, no. 12, pp. 1501–1505, Dec. 2014.

[3] L. Dai, B. Wang, Y. Yuan, S. Han, C.-L. I, and Z. Wang, "Non-orthogonal multiple access for 5G: Solutions, challenges, opportunities, and future research trends," *IEEE Commun. Mag.*, vol. 53, no. 9, pp. 74–81, Sep. 2015.

[4] J. Choi, "Non-orthogonal multiple access in downlink coordinated two-point systems," *IEEE Commun. Lett.*, vol. 18, no. 2, pp. 313–316, Feb. 2014.

[5] Z. Ding, M. Peng, and H. V. Poor, "Cooperative non-orthogonal multiple access in 5G systems," *IEEE Commun. Lett.*, vol. 19, no. 8, pp. 1462–1465, Aug. 2015.

[6] J.-B. Kim and I.-H. Lee, "Capacity analysis of cooperative relaying systems using non-orthogonal multiple access," *IEEE Commun. Lett.*, vol. 19, no. 11, pp. 1949–1952, Nov. 2015.

[7] J.-B. Kim and I.-H. Lee, "Non-orthogonal multiple access in coordinated direct and relay transmission," *IEEE Commun. Lett.*, vol. 19, no. 11, pp. 2037–2040, Nov. 2015.

[8] Y. Xu, H. Sun, R. Q. Hu, and Y. Qian, "Cooperative non-orthogonal multiple access in heterogeneous networks," in *Proc. IEEE Global Commun. Conf. (GLOBECOM)*, Dec. 2015, pp. 1–6.

[9] M. Xu, F. Ji, M. Wen, and W. Duan, "Novel receiver design for the cooperative relaying system with non-orthogonal multiple access," *IEEE Commun. Lett.*, vol. 20, no. 8, pp. 1679–1682, Aug. 2016.

[10] R. Jiao, L. Dai, J. Zhang, R. MacKenzie, and M. Hao, "On the performance of NOMA-based cooperative relaying systems over Rician fading channels," *IEEE Trans. Veh. Technol.*, vol. 66, no. 12, pp. 11409–11413, Dec. 2017.

[11] D. Wan, M. Wen, F. Ji, Y. Liu, and Y. Huang, "Cooperative NOMA systems with partial channel state information over Nakagami-*m* fading channels," *IEEE Trans. Commun.*, vol. 66, no. 3, pp. 947–958, Mar. 2018.

[12] B. Zheng, M. Wen, E. Basar, and F. Chen, "Multiple-input multiple-output OFDM with index modulation: Low-complexity detector design," *IEEE Trans. Signal Process.*, vol. 65, no. 11, pp. 2758–2772, Jun. 2017.

[13] M. Wen, E. Basar, Q. Li, B. Zheng, and M. Zhang, "Multiple-mode orthogonal frequency division multiplexing with index modulation," *IEEE Trans. Commun.*, vol. 65, no. 9, pp. 3892–3906, Sep. 2017.

[14] H. Xie, F. Gao, S. Jin, J. Fang, and Y.-C. Liang, "Channel estimation for TDD/FDD massive MIMO systems with channel covariance computing," *IEEE Trans. Wireless Commun.*, vol. 17, no. 6, pp. 4206–4218, Jun. 2018.

[15] Y. Liu, G. Pan, H. Zhang, and M. Song, "On the capacity comparison between MIMO-NOMA and MIMO-OMA," *IEEE Access*, vol. 4, pp. 2123–2129, 2016.

[16] W. Feng, Y. Wang, D. Lin, N. Ge, J. Lu, and S. Li, "When mmWave communications meet network densification: A scalable interference coordination perspective," *IEEE J. Sel. Areas Commun.*, vol. 35, no. 7, pp. 1459–1471, Jul. 2017.

[17] B. Wang, F. Gao, S. Jin, H. Lin, and G. Y. Li, "Spatial- and frequency-wideband effects in millimeter-wave massive MIMO systems," *IEEE Trans. Signal Process.*, vol. 66, no. 13, pp. 3393–3406, Jul. 2018.

[18] R. Zhang, Z. Zhong, J. Zhao, B. Li, and K. Wang, "Channel measurement and packet-level modeling for V2I spatial multiplexing uplinks using massive MIMO," *IEEE Trans. Veh. Technol.*, vol. 65, no. 10, pp. 7831–7843, Mar. 2016.

[19] Y. Chen, L. Wang, Y. Ai, B. Jiao, and L. Hanzo, "Performance analysis of NOMA-SM in vehicle-to-vehicle massive MIMO channels," *IEEE J. Sel. Areas Commun.*, vol. 35, no. 12, pp. 2653–2666, Dec. 2017.

[20] J.-B. Kim, I.-H. Lee, and J.-H. Lee, "Capacity scaling for D2D aided cooperative relaying systems using NOMA," *IEEE Commun. Lett.*, vol. 7, no. 1, pp. 42–45, Feb. 2018.

[21] W. Feng, J. Wang, Y. Chen, X. Wang, N. Ge, and J. Lu, "UAV-aided MIMO communications for 5G Internet of Things," *IEEE Internet Things J.*, vol. 6, no. 2, pp. 1731–1740, Apr. 2019.

[22] T. Qi, W. Feng, and Y. Wang, "Outage performance of non-orthogonal multiple access based unmanned aerial vehicles satellite networks," *China Commu.*, vol. 15, no. 5, pp. 1–8, May 2018.

[23] X. Lai, L. Fan, X. Lei, J. Li, N. Yang, and G. K. Karagiannidis, "Distributed secure switch-and-stay combining over correlated fading channels," *IEEE Trans. Inf. Forensics Security*, vol. 14, no. 8, pp. 2088–2101, Aug. 2019.

[24] C. Li, W. Zhou, K. Yu, L. Fan, and J. Xia, "Enhanced secure transmission against intelligent attacks," *IEEE Access*, vol. 7, pp. 53596–53602, 2019.

[25] Z. Ding, H. Dai, and H. V. Poor, "Relay selection for cooperative NOMA," *IEEE Wireless Commun. Lett.*, vol. 5, no. 4, pp. 416–419, Aug. 2016.

[26] Z. Yang, Z. Ding, Y. Wu, and P. Fan, "Novel relay selection strategies for cooperative NOMA," *IEEE Trans. Veh. Technol.*, vol. 66, no. 11, pp. 10114–10123, Nov. 2017.

[27] D. Deng, L. Fan, X. Lei, W. Tan, and D. Xie, "Joint user and relay selection for cooperative NOMA networks," *IEEE Access*, vol. 5, pp. 20220–20227, 2017.

[28] J. Zhao, Z. Ding, P. Fan, Z. Yang, and G. K. Karagiannidis, "Dual relay selection for cooperative NOMA with distributed space time coding," *IEEE Access*, vol. 6, pp. 20440–20450, 2018.

[29] P. Xu, Z. Yang, Z. Ding, and Z. Zhang, "Optimal relay selection schemes for cooperative NOMA," *IEEE Trans. Veh. Technol.*, vol. 67, no. 8, pp. 7851–7855, Aug. 2018.

[30] Y. Liu, Z. Ding, M. Elkashlan, and H. V. Poor, "Cooperative non-orthogonal multiple access with simultaneous wireless information and power transfer," *IEEE J. Sel. Areas Commun.*, vol. 34, no. 4, pp. 938–953, Apr. 2016.

[31] X. Yue, Y. Liu, S. Kang, A. Nallanathan, and Z. Ding, "Spatially random relay selection for full/half-duplex cooperative NOMA networks," *IEEE Trans. Commun.*, vol. 66, no. 8, pp. 3294–3308, Aug. 2018.

[32] S. Timotheou and I. Krikidis, "Fairness for non-orthogonal multiple access in 5G systems," *IEEE Signal Process. Lett.*, vol. 22, no. 10, pp. 1647–1651, Oct. 2015.

[33] P. Xu and K. Cumanan, "Optimal power allocation scheme for non-orthogonal multiple access with α-fairness," *IEEE J. Sel. Areas Commun.*, vol. 35, no. 10, pp. 2357–2369, Oct. 2019.

[34] W. Duan, J. Ju, J. Hou, Q. Sun, X.-Q. Jiang, and G. Zhang, "Effective resource utilization schemes for decode-and-forward relay networks with NOMA," *IEEE Access*, vol. 7, pp. 51466–51474, 2019.

[35] J. Ju, G. Zhang, Q. Sun, L. Jin, and W. Duan, "On the performance of receiver strategies for cooperative relaying cellular networks with NOMA," *Eurasip J. Wireless Commun. Netw.*, vol. 2019, Mar. 2019, Art. no. 67. doi: 10.1186/s13638-019-1377-5.

[36] I. S. Gradshteyn and I. M. Ryzhik, *Table of Integrals, Series and Products*, 7th ed. New York, NY, USA: Academic, 2007.